

Amplification of an ultrashort pulse laser by stimulated Raman scattering of a 1 ns pulse in a low density plasma

R. K. Kirkwood, E. Dewald, C. Niemann, N. Meezan, S. C. Wilks,
D. W. Price, and O. L. Landen

*University of California, Lawrence Livermore National Laboratory, P.O. Box 808, Livermore,
California 94551, USA*

J. Wurtele, A. E. Charman, and R. Lindberg

University of California at Berkeley/Lawrence Berkeley Laboratory, Berkeley, California 94720, USA

N. J. Fisch, V. M. Malkin, and E. O. Valeo

Princeton University, PO Box 451, Princeton, New Jersey 08543, USA

(Received 14 February 2007; accepted 9 October 2007; published online 27 November 2007)

Experiments are described in which a 1 mJ, 1 ps, 1200 nm seed laser beam is amplified by the interaction with an intersecting 350 J, 1 ns, 1054 nm pump beam in a low density ($1 \times 10^{19}/\text{cm}^3$) plasma. The transmission of the seed beam is observed to be enhanced by $\geq 25\times$ when the plasma is near the resonant density for stimulated Raman scattering, compared to measured transmissions at wavelengths just below the resonant value. The amplification is observed to increase rapidly with increases in both pump intensity and plasma density. © 2007 American Institute of Physics. [DOI: [10.1063/1.2804083](https://doi.org/10.1063/1.2804083)]

I. INTRODUCTION

Generation of ultrahigh power laser pulses with picosecond or shorter duration is of interest for a wide variety of applications including, inertial confinement fusion,¹ x-ray radiography of dense material,² and particle acceleration.³ Present techniques use the compression of a much longer, frequency chirped pulse by solid state optics,⁴ and find the maximum power achievable is determined by the material damage limits of the final optic. Theoretical investigations have considered compressing pulses by using a short pulse to seed the stimulated Raman scatter (SRS) of a long pulse pump.^{5,6} The principle advantage of this approach is that the high power density is produced in a plasma that does not suffer the damage limits of solid state optics, and the possibility of compressing pulses of tens of ps duration to produce powers approaching the exawatt (10^{18} W) level using plasmas has been discussed in previous work.⁵ The pulse compression approach is to produce a sufficiently large density perturbation by the “beat” ponderomotive force of the two beams, that the perturbation scatters nearly all the incident pump power. When the beams interact in a counterpropagating (backscatter) geometry it will also be possible to transfer the energy of much longer pulses into the counterpropagating short pulse, provided the plasma is long enough to allow complete interaction of the two pulses ($l \sim c/2 \tau_{\text{long}}$ or 15 cm per ns compressed). The power transferred and amplification rate of the short pulse beam can be maximized by taking advantage of the resonant SRS instability to minimize the needed pump and seed intensity.⁵ That is, the seed beam wavelength can be adjusted to seed SRS in a plasma which has low enough density that inverse bremsstrahlung absorption of the beam is sufficiently small for the desired plasma size. Recent experiments testing the concept for the compression of ≈ 100 ps pump pulses to < 1 ps durations have

shown large amplification of short pulses can be achieved in cold laser produced plasmas^{7–10} where the product of plasma wave number and Debye length ($k\lambda_D$) remains small for the brief duration of the experiment.

To achieve efficient compression of longer pulses with durations up to 1 ns, however, the scattering wave will have to be driven to a large amplitude in a plasma that can coexist with the pump and will not significantly absorb the beams over longer, multi-cm spatial and ns time scales. Since the pump has to be intense enough and the plasma dense enough to allow SRS driven waves to grow to large enough amplitudes that they scatter most of the pump energy, the inverse bremsstrahlung heating of the plasma by the pump over its entire pulse length will cause the electron temperature to be significantly higher than in previous studies where amplification by < 100 ps length pulses was demonstrated^{7–10} and the plasma heating only occurred for < 100 ps. Also, as the plasma length is increased toward the 15 cm size needed to compress 1 ns pulses, the inverse bremsstrahlung absorption will need to be kept low by maintaining low plasma density. Although the lower density will lessen the heating, when taken together, these two effects of the 1 ns pump cause greater heating and a tendency toward higher temperatures, as well as lower density relative to experiments with shorter duration pumps; both cause increased values of the $k\lambda_D$ product which leads to larger damping for linear waves, and a reduced linear wave response as well as modifying the eventual nonlinear state of the wave. Because pulse compression will require that the Langmuir wave grow large from a very small initial amplitude the plasma must have a sufficiently large linear response to the ponderomotive force to produce significant linear SRS gain. This requirement leads to an upper limit on the $k\lambda_D$ product in the range of 0.5–1.0. The wave damping may then be increased above its linear value as the wave amplitudes grow large, leading to a reduc-

tion in the SRS growth rate, which in the strong damping limit is inverse with the damping rate.¹¹ Any nonlinear enhancement to the damping can be compensated for to some extent by allowing growth to occur over a larger fraction of the plasma length prior to reaching pump depletion. In any case, a significant growth rate for the linear waves will certainly be necessary for pulse compression. For these reasons the acceptable range of plasma conditions will also be limited by the need for low $k\lambda_D$.

In this work we identify a region in density and temperature space in which the dual requirements of moderate linear wave damping and moderate inverse bremsstrahlung absorption of the light waves can be satisfied to allow Langmuir waves to grow to the nonlinear regime needed for compression of 1 ns pulses and for efficient propagation of the electromagnetic waves and show that the needed plasma conditions can coexist with a pump beam intense enough to produce SRS gain. In particular, a window in plasma temperature and density in the range of a few $10^{18}/\text{cm}^3$ to $10^{19}/\text{cm}^3$ electron density and of <300 eV electron temperature, is identified as satisfying the absorption and linear wave growth requirements for a 1 micron wavelength beam. For example, a 15 cm long hydrogen plasma interacting with a 1054 nm pump beam, will simultaneously achieve $<20\%$ absorption of each of the 1 micron wavelength pulses by inverse bremsstrahlung, and $k\lambda_D=0.44$ for weak linear wave damping (i.e., $\nu/\omega < 0.073$ for undriven waves) when the electron temperature is ~ 275 eV and the electron density is $n_0 \sim \times 10^{19}/\text{cm}^3$. At the same time scattering 100% of the pump power in this plasma will require a wave amplitude of $dn \geq 1 \times 10^{18}/\text{cm}^3 \sim 0.1 \times n_0$ (higher if the wave is significantly incoherent) which is a fraction of the average density. Plasmas in this regime are attractive for compression of 1 ns pulses, if such a plasma can also coexist with the needed pump, if the nonlinear effects on the Langmuir wave do not prevent the waves from growing to the amplitude needed to deplete the pump and seed beams, and if the competing plasma instabilities can be suppressed. The successful compression of the 1 ns pulse to ~ 1 ps in such a plasma will not only provide higher power but also high power density when the amplified beam can be brought to smaller focus, which can be accomplished by the amplification of a focusing seed beam, and may be further enhanced by a second Raman amplifier to reduce the beam spot size as discussed in Ref. 12.

This paper describes the first demonstration of amplification of a 1 ps beam by seeding the SRS of a 1 ns pump beam, in a plasma with sufficiently small inverse bremsstrahlung absorption for efficient compression of the pump, that is, with a density $\leq 1\%$ of critical and a temperature produced by heating by the 1 ns pump. The amplification rate of the low amplitude seed, and total scattered power observed in the configuration shown in Fig. 1 are found to be similar to predictions of particle in cell (PIC) simulations for seeded SRS in the plasma, demonstrating that a low amplitude seed can be amplified to large amplitude in the plasma conditions produced by the pump.

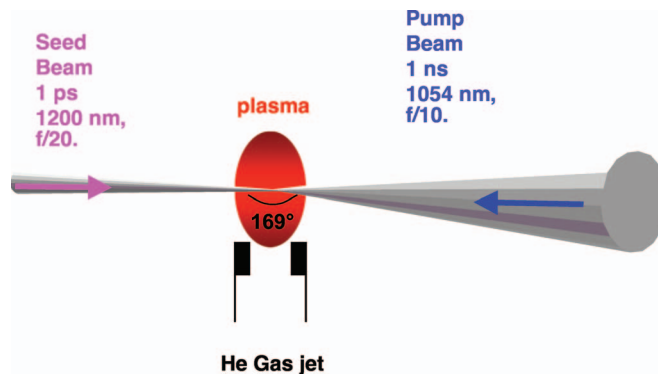


FIG. 1. (Color) Experimental setup showing the 350 J, 1 ns, pump beam and the 1 ps seed crossing at 11° away from counterpropagating in a He plasma formed by interaction of the pump with a gas jet.

II. PLASMA FORMATION AND UNSEEDED SRS EXPERIMENTS

The experiments were carried out on the Janus/Comet laser facility, using a 100–350 J, 1 ns duration, pump beam produced at the 1054 nm wavelength. The pump beam was $f/10$ and had its spot conditioned with a phase plate¹³ to produce a 200 micron diameter flat top intensity profile, which was focused onto a He gas jet target as shown as the pump beam and plasma in Fig. 1. The initial He gas density was made uniform over a region ≥ 2 mm by passing the gas through a transonic nozzle similar to what has been described in Ref. 14 and is adjustable over a range that allows the initial electron densities in the interaction region to vary between $2.5 \times 10^{18}/\text{cm}^3$ and $10^{19}/\text{cm}^3$. The plasma was formed by the pump beam which ionized and heated the gas.

Expected plasma conditions were studied with simulations using the HYDRA code¹⁵ which are shown in Fig. 2 and indicate that the electron density of the plasma is initially determined by the gas density and has a profile that is initially uniform along the axis of the laser and transversely uniform over the region of the focal spot. Throughout the pump pulse, the plasma has a transverse width that is much larger than the laser spot size because of thermal conduction out of that region. Earlier experiments and simulations which include nonlocal electron heat transport have shown that the actual profile width may be even wider than HYDRA predicts.¹⁶ The axially uniform density profile is needed to maintain the resonance with the seed beam over a long interaction length and is maintained for most of the 1 ns duration of the pump. In fact the simulations show that the density, and the homogeneity begin to decrease, due to plasma expansion later in the heater pulse, and, for the conditions studied here, axial uniformity is maintained to better than 10% over a 2 mm plateau for $t < 800$ ps. The peak electron temperatures, determined from the simulations, are 155 eV for the case of $2.5 \times 10^{18}/\text{cm}^3$ and 350 J incident, 210 eV for the case of $1 \times 10^{19}/\text{cm}^3$, and 115 J incident, and 275 eV for the case of $10^{19}/\text{cm}^3$ and 350 J incident. The corresponding values of $\kappa\lambda_{\text{Debye}}$ for the Langmuir wave driven by the beat of the 1056 nm pump and the resonant seed beam for these simulated conditions are: 0.67, 0.38, 0.43, respectively. Because the simulation does not include nonlocal effects in the

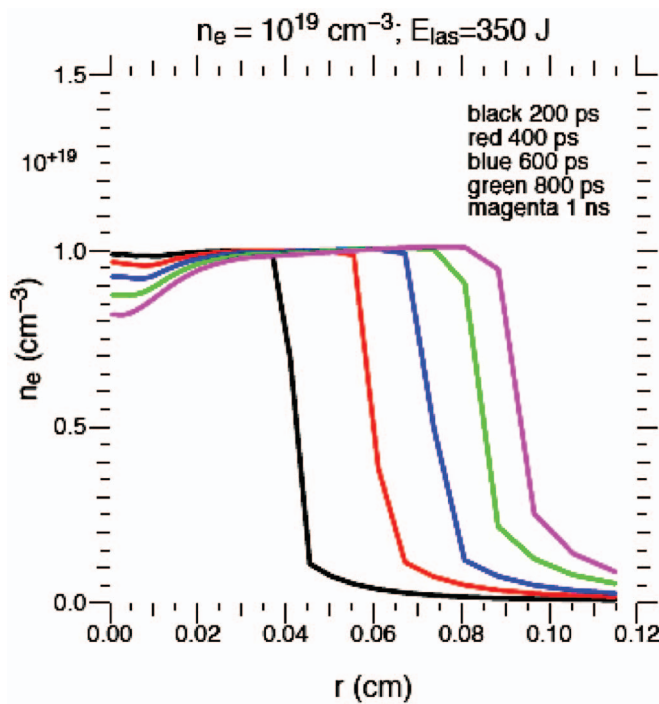


FIG. 2. (Color) Simulations of plasma conditions at different times show that the plasma density varies by less than 17% over the 1 ns pump duration and has a transverse gradient scale that is much larger than the 200 micron diameter laser spot.

heat transport, which as shown in Ref. 16 can make the electron temperature somewhat lower at the peak of the profile the actual values of $k\lambda_{\text{Debye}}$ may be somewhat smaller.

The plasma axial, and transverse density profiles, were confirmed to have the expected uniform plateau which was first demonstrated in Ref. 14, by a series of single beam experiments with a ~ 350 J pump beam energy, incident on a He gas jet produced by 3 mm and 4 mm diameter nozzles, by using a 527 nm wavelength, imaging interferometer that viewed the plasma normal to the pump beam axis and gas jet axis. The profiles of line integrated density for both jet diameters were flat to better than the 20% measurement accuracy of the system over a distance > 2 mm as expected. During these single beam experiments the SRS light that grows from plasma fluctuations and propagates in the direction 11° away from counterpropagating with the pump (corresponding to the direction of the seed beam in two beam experiments), is collected by an $\sim f/10$ optic and passed through a beamsplitter to a calorimeter to measure the nearly backscattered energy. The signal from the splitter is reimaged into a spectrometer with a InP charged coupled device based camera that recorded the transmitted spectrum in the range of 1040–1230 nm which is calibrated by the calorimetric measurement.

The measured spectrum is shown in Fig. 3 for the 3 mm diameter nozzle with six different values of backing gas pressure (measured behind the gas jet valve just prior to its opening). The data shows that the wavelength of peak SRS increases with the backing pressure consistent with the plasma density being approximately proportional to backing pressure at high pressure. The highest pressure case shown

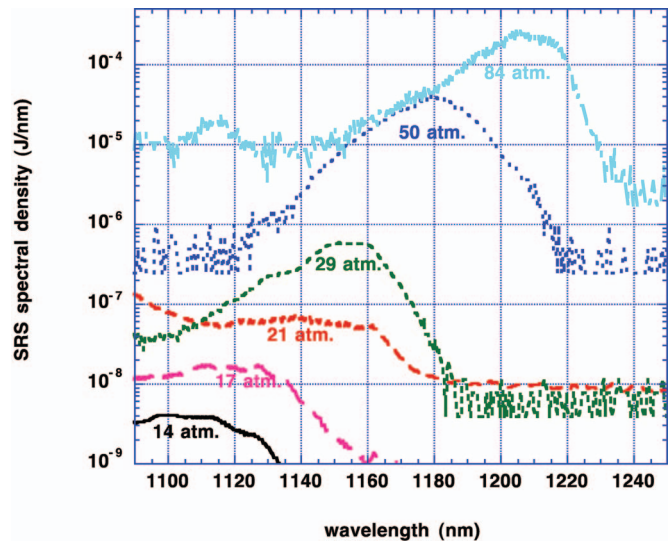


FIG. 3. (Color) Measurement of the unseeded SRS scatter produced by the pump and collected in the solid angle which the seed beam will occupy, showing an increase in wavelength of peak scattering, along with a dramatic increase in magnitude of the scattering, as the plasma density is increased by increasing the backing pressure of the jet.

had similar conditions to experiments where the electron density was verified to be $1 \times 10^{19} \text{ cm}^{-3}$ using the imaging interferometer, and the wavelength of the peak of the scattered spectrum confirms this value of electron density. However because the ratio of the measured backing pressure to the plasma density in the interaction region is not expected to be precisely constant, and also is sensitive to the area of the open valve orifice, and the distance from the valve to the nozzle, which both were adjusted somewhat between the interferometric experiments and the single beams scattering experiments shown, the peak wavelength of the observed SRS spectrum is a more accurate measure of the plasma density than the backing pressure. As a result, to achieve best resonance with the seed in the two beam experiments described below, we adjust the backing pressure so that the measured wavelength of the peak of the unseeded SRS spectrum matches the seed wavelength, and do not rely on direct density or pressure measurements. The observation that the SRS spectrum at the highest density has a full width at the half maximum (FWHM) of ~ 30 nm corresponding to an $\sim 17\%$ frequency width for the scattering Langmuir wave, which is greater than would be expected for a gain narrowed SRS resonance at this value of $k\lambda_{\text{Debye}}$ (for which the Langmuir wave damping rate is only 7.3% of the real frequency), suggests that the beam is interacting over a region with density inhomogeneities. This is likely due to the nonuniformity present in the gas density at the edges of the jet as well as to density perturbations produced by the beam heating and ponderomotive force. The data of Fig. 3 also shows that the observed level of the scattering by unseeded waves increases dramatically, both with increased backing pressure, and with increases in the wavelength of peak scattering over the range of 1124–1200 nm. This is consistent with the SRS scattering increasing rapidly as the plasma density increases from $2.3 \times 10^{18} / \text{cm}^3$ to $1 \times 10^{19} / \text{cm}^3$ as expected because SRS gain

rate increases dramatically at high density, in part due to reduced Debye length.

III. RESULTS WITH A 1 ps BEAM SEEDING THE SRS OF THE PUMP BEAM

The laser used for the seed beam delivered 10–20 mJ in 1 ps, also at 1054 nm wavelength and was converted to circular polarization and passed through a high pressure (600 psi) H₂ Raman cell to convert to up to a few mJ in both 1124 nm and ~1200 nm lines via interaction with the H₂ Raman resonance at first and second order. The seed beam is coupled to the target at an 11° angle away from counter-propagating with the pump with an *f* number of 20 as shown in Fig. 1, and focused at a point 3.5 mm before it intersects the pump to ensure that the spot size is close to that of the pump at the point of intersection. This beam pointing and crossing angle allows the seed to interact with the pump along a 1 mm path where the plasma is most homogenous. The circular polarization of the seed is needed in the high pressure cell to excite the desired rotational Raman resonance in the gas. Allowing the beam to maintain circular polarization in the plasma also ensures all of the seed energy that is aligned to the linear pump polarization is available in the target and that the aligned component of the seed energy is 50% of the total. The seed energy is collected and measured by a similar system used to detect the scattered light in the single beam experiments.

Initial experiments with both seed and pump beams incident on a jet of He gas with $10^{19}/\text{cm}^3$ electron density were carried out at the reduced pump energy and intensity of 115 J and $3.5 \times 10^{14} \text{ W/cm}^2$, to minimize the unseeded SRS backscatter produced by the pump and to make the transmitted signal of the amplified seed well above the background of unseeded scattering. The pump was intersected by the seed with 174 μJ of seed energy in the 1165–1220 nm spectral range, in three cases: (1) pump and seed with seed beam arriving 400 ps into the pump pulse, (2) pump and seed with the seed beam arriving at 1.0 ns (after the pump has ramped down), (3) seed beam only as shown in Fig. 4. A fourth case with no seed, (4) pump beam only, is also shown in Fig. 4.

To allow a quantitative measure of the amplification from the spectral transmission measurements shown in Fig. 4, the spectra are reduced to energy measurements for all the cases discussed below by integrating over the same 1165–1220 nm range. The first case, in which the seed and pump are coincident in time shows significantly larger transmitted spectral density and energy than either the second case with the pump and delayed seed or the third case with the seed alone. The amplification of the seed total transmitted energy in the first case is $2.6\times$ compared to the third case of seed only (vacuum), when the spectra are integrated over 1165–1220 nm. The transmitted energy in the first case is also $3.2\times$ higher than the energy collected in the second case when the seed and pump are both present but the seed is late enough not to interact with the pump as well as the essentially identical fourth case when only the pump is present. The polarization dependence of the spectrometer sensitivity is negligible in these experiments because it is operated with

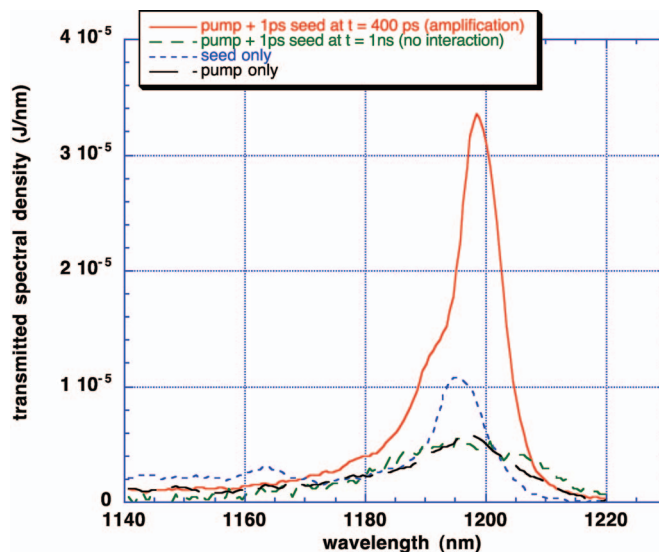


FIG. 4. (Color) Transmitted spectrum of 1 ps seed beam in a $1 \times 10^{19}/\text{cm}^3$ He plasma produced by a $3.5 \times 10^{14} \text{ W/cm}^2$ pump, showing amplification of the spectrum when the seed arrived 400 ps into the pump pulse, compared either to the case with the seed arriving at 1 ns after the pump turns off or to the seed beam alone. The amplified seed level is well above the background scattering shown for the pump beam only.

incidence angles on the grating that are close to normal. This insensitivity to seed polarization has also been confirmed by comparison of the integrated signals detected by the spectrometer and those detected by the polarization independent calorimeter which are seen to track well in the cases studied. Attenuation of the seed is indicated by the fact that the delayed seed case shows a spectrum very similar to the thermal SRS spectrum produced by the pump alone. As a result of this the actual amplification of the seed beam is even greater than the above numbers indicate, since the unamplified seed is being attenuated by the plasma, both by inverse bremsstrahlung absorption and loss of energy outside the collection cone. The attenuation of the seed beam due to inverse bremsstrahlung is more significant in these experiments because the seed crosses the pump beam at a small angle and propagates a significant distance in the cold plasma that is created well outside of the pump beam region by heat and particle transport. The simulations discussed below predict a $0.93\times$ attenuation (7% absorption) in the 2 mm distance, due to inverse bremsstrahlung, but the magnitude of the absorption in the wings of the profile may be very sensitive to the exact temperature and density profiles in the wings which are difficult to simulate. In addition some large fraction of the measured attenuation in the experiments may also be due to seed energy being refracted or scattered out of the detection cone by small scale plasma density fluctuations which are also not included in the simulation. This attenuation was most accurately determined quantitatively in the experiments in Fig. 4 by a simultaneous measurement of the attenuation of a 1124 nm line also present in the seed beam. The 1124 nm line was produced in the H₂ Raman cell with a similar intensity to the 1200 nm line, and transported to the plasma and detection spectrometer in the seed beam optics, and provides a measurement of the attenuation produced by the plasma for

a beam that is not resonant with Langmuir waves and therefore is unamplified. The 1124 nm line shows an attenuation of $2.44\times$ when comparing the experiment of case 3 to case 1, which, since the refraction and attenuation of the beam is expected to change little with the small change in wavelength, indicates that the unamplified seed would be attenuated by approximately the same factor. When the amplified seed energy (case 1) is reduced by the unseeded SRS energy of the pump (case 4) and compared to the seed only vacuum (case 3) reduced by the measured attenuation at 1124 nm, the overall amplification of the seed energy in this case is $4.4\times$ at this pump intensity and beam timing. Note that the values of measured amplification discussed above and in the remainder of the paper are calculated as the amplification relative to the energy in the circularly polarized seed beam. If the seed were linearly polarized and its polarization was aligned to the pump with the alignment maintained throughout the interaction volume, the amplifications observed would be expected to be approximately double our experimental values because only the aligned component of the energy is amplified by SRS in the experiments. However, we present the actual measured values of amplification relative to the incident circularly polarized energy rather than extrapolating to include this possible enhancement because it is difficult to quantify how well an aligned, linear polarization could be maintained throughout the inhomogeneous plasma we study.

To study the dependence of the observed amplification on the intensities and timing of the beams, a second set of experiments was carried out with higher pump intensity and with two different relative delays in pump and seed timing. The first of these had a seed delay of 700 ps with respect to the pump, a seed energy of $285\ \mu\text{J}$ and a pump energy and intensity of $350\ \text{J}$ and $1.1\times 10^{15}\ \text{W}/\text{cm}^2$. With these parameters cases (1)–(3) above were repeated, and are shown in Fig. 5. The total transmitted energy in the resonant case (case 1) is $\approx 6.7\ \text{mJ}$ which is $23.5\times$ higher than the seed only case, and is $1.76\times$ higher than the energy collected when the seed and pump are both present but the seed is late enough not to interact with the pump (cases 1 and 2). The attenuation of the off resonant 1124 nm line of the seed was determined from measurements in the same manner as previously, and is found to be $3.7\times$. This indicates that when the amplified seed energy (case 1) is reduced by the unseeded SRS energy of the pump (case 2) and compared to the unamplified seed (case 3) corrected for the measured attenuation at 1124 nm, the overall amplification of the seed energy in this case is $37\times$ at this pump intensity and beam timing.

The second, high intensity experiment had a seed delay of 240 ps, seed energy of $259\ \mu\text{J}$, and a pump energy and intensity of $350\ \text{J}$ and $1.1\times 10^{15}\ \text{W}/\text{cm}^2$. For this experiment, in addition to an advanced timing for the seed beam, small adjustments to the position and the area of the collection optic of the transmitted seed energy were made, which reduced the collection of the unseeded, or “background,” SRS scatter from the pump and increased the fraction of the transmitted seed energy that was collected when the plasma was present. These adjustments served to decrease the unwanted signal from unseeded SRS scatter, as well as study

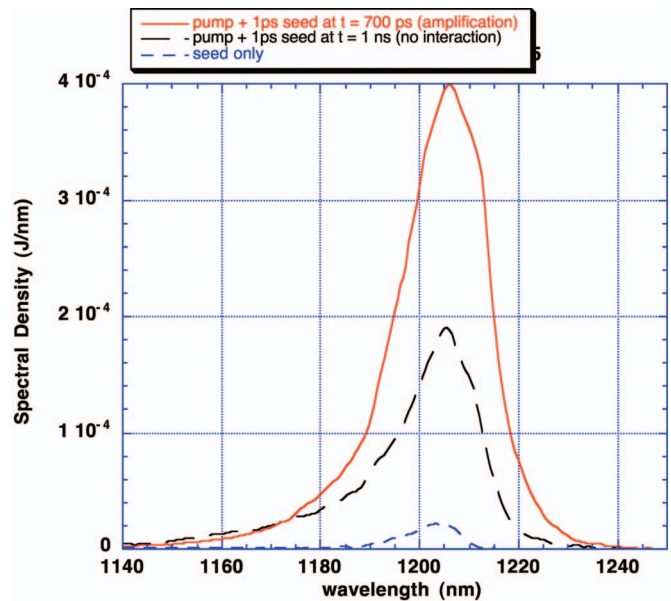


FIG. 5. (Color) Transmitted spectrum for the seed alone and pump and seed together with seed timing adjusted for both interaction and no-interaction as in Fig. 4 but with a $1.1\times 10^{15}\ \text{W}/\text{cm}^2$ pump beam intensity, and a seed arrival time of 700 ps.

the time dependence of the amplification. Again cases (1)–(3) above were repeated for these new conditions, and the results are shown in Fig. 6. From the measured spectra the total transmitted energy in the resonant case (case 1) is found to be $2.96\ \text{mJ}$ which is $11.4\times$ higher than the seed only case, and is $2.4\times$ higher than the energy collected when the seed and pump are both present but the seed is late enough not to interact with the pump (cases 1 and 2). The attenuation of the off resonant 1124 nm line of the seed was also determined from measurements and found to be $2.39\times$. This indicates that when the amplified seed energy (case 1) is reduced by

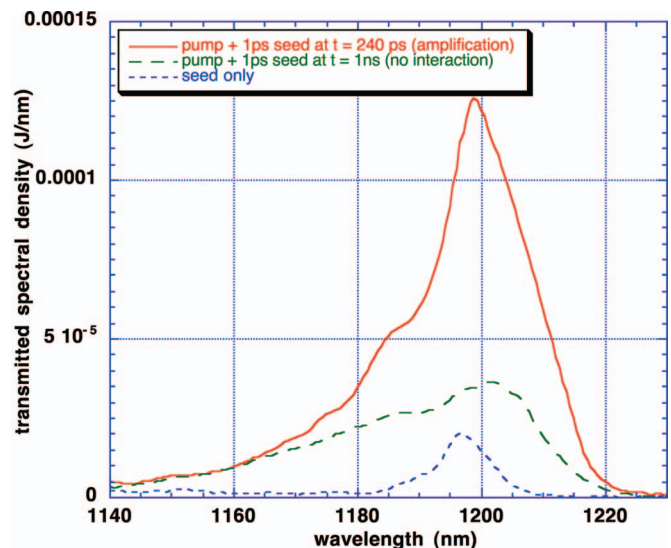


FIG. 6. (Color) Transmitted spectrum for the seed alone and pump and seed together with seed timing adjusted for both interaction and no-interaction as in Fig. 4 but with a $1.1\times 10^{15}\ \text{W}/\text{cm}^2$ pump beam intensity, and a seed arrival time of 240 ps.

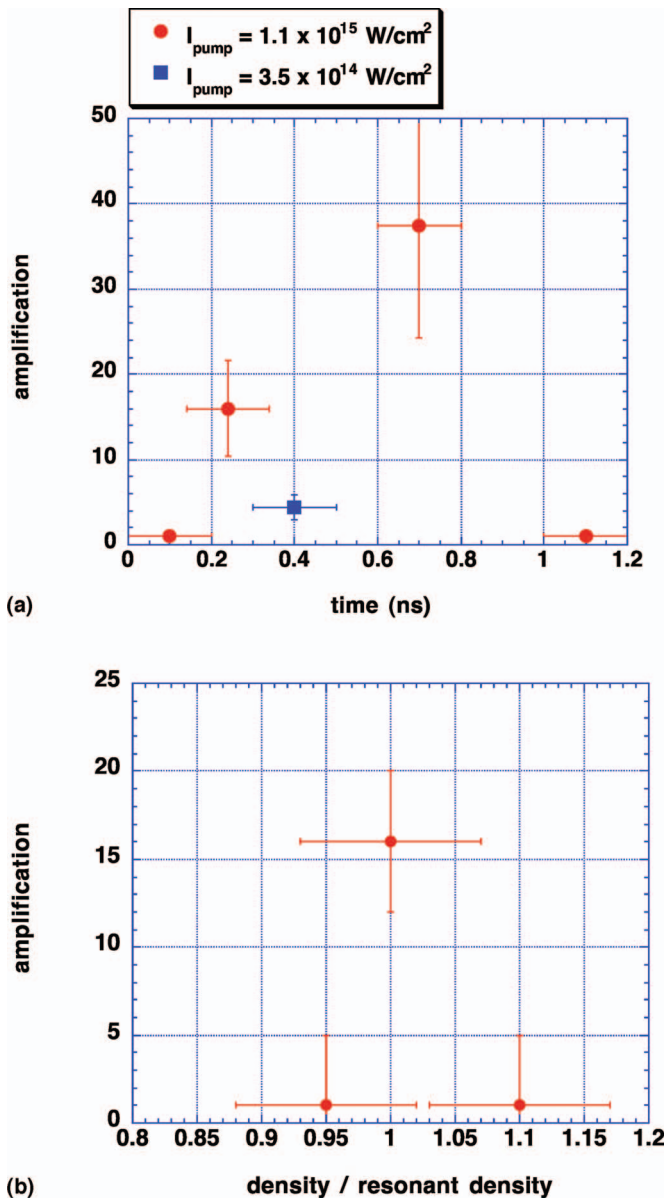


FIG. 7. (Color) (a) The measured seed amplification relative to an unamplified seed (as described in the text) is plotted vs arrival time of the seed relative to the start of the 1 ns pump pulse, for two different pump intensities. (b) Plot of seed amplification vs initial plasma density for the high intensity pump case, showing a peak near the resonant value of plasma density.

the unseeded SRS energy of the pump (case 2) and compared to the unamplified seed (case 3) corrected for the measured attenuation, the overall amplification of the seed energy in this case is $16.0\times$ at this pump intensity and beam timing. A summary of the observed amplification for three cases described in Figs. 4–6 and two additional experiments at early and late time is shown in Fig. 7(a). This collection of data shows that significant amplification is observed over the central period of the pump pulse (200–700 ps) while amplification vanished at early and late time when the pump intensity is substantially reduced as expected. The two points at high pump intensity also suggest that the amplification increases with time during the pulse, which may be due to small changes in the plasma and beam conditions during the pump

pulse modifying the resonance matching of the beams. A comparison of the amplifications observed at different pump intensities during the central period of the pulse also provide an indication of a significant intensity dependence of the amplification.

Further experiments were done at the increased pump intensity to determine the dependence of the amplification on the initial electron density, by varying the pressure in the gas jet while maintaining the seed timing between 200 ps and 700 ps and other conditions similar to the cases shown in Figs. 5 and 6, the results of which are shown in Fig. 7(b). The results indicate that the amplification is sharply resonant with the plasma initial density, with the peak amplification occurring near the density at which the plasma frequency equals the frequency separation of the pump and seed, as expected from the frequency and wave-number matching conditions.

The amplifications observed are similar to what is obtained from PIC simulations under similar plasma and beam conditions. 1D simulations were performed for a uniform plasma with the density adjusted near the linear Langmuir wave resonance, for 1200 nm light, and the electron temperature as determined from the fluid simulations. A 1 ns pump beam with a $1.1 \times 10^{15} \text{ W/cm}^2$ counterpropagated with a seed beam with a step pulse shape with a <1 ps rise time and an intensity of $\approx 0.5\%$ of the pump. These values represent the experimental situation when the pump energy is 350 J and the seed energy is 1.7 mJ. The seed amplitude was measured after a 250 micron propagation distance and the square of the ratio to the incident amplitude indicated the power gain achieved. It was found that the gain peaked at $140\times$ near 0.013 of critical density and remained above $\frac{1}{2}$ that value in separate simulations with densities between 0.011 and 0.017 critical and that the output pulse remained high for the ≈ 1 ps duration of the experimental pulse for this case. The fact that the seed intensity approaches the pump intensity in only 250 microns indicates that the SRS gain rate is sufficient that subsequent wave propagation and growth of the seed that would occur in the multi-cm plasma length needed for ns pulse compression would cause a large fraction of the pump pulse length to be compressed to the ps time scale. These 1D simulations do not include the effects of the polarization of a vector field and correspond to aligned, linear polarizations. However, the result can be compared to the measurements by assuming that a circularly polarized field would only have $\frac{1}{2}$ its energy interacting with the pump so the simulated amplification for a circularly polarized beam would be reduced from $140\times$ to $\sim 69\times$ at maximum. These values show a somewhat broader resonance than observed in the experimental data in Fig. 7(b), which may reflect actual experimental temperature that are somewhat lower than the simulated values which leads to lower wave damping and a narrower resonance in the experiments. The reduction in the simulated transmission of the seed after 1 ps when the incident seed amplitude is still high may reflect a shortening of the pulse as has been discussed in other contexts.⁵ In summary, these simulations show the resonant excitation of the Langmuir waves and amplification of the seed beam when the plasma conditions are similar to those in the experiments.

The experimental gains are somewhat lower than the simulations which may result from, resonance detuning by plasma inhomogeneity induced by the pump beam (which is not included in the fluid simulations which determined the interaction length), and by higher dimensional saturation effects of the large amplitude Langmuir waves.

A third set of experiments was done at these beam intensities and several electron densities in the vicinity of $2.3 \times 10^{18}/\text{cm}^3$, to allow the 1124 nm line produced in the Raman gas cell to resonantly seed the plasma Raman scattering. In these experiments, the unseeded SRS was much reduced so the seed energy could be reduced by 10^5 and still remain above the unseeded scattering, allowing the amplification to be measured at much lower wave amplitude to avoid any saturation of the amplifying plasma waves that might occur at these reduced plasma densities. The amplified transmitted seed energy was never different from the unamplified value by significantly more than the measurement uncertainty (which is caused primarily by small variations in the seed energy from shot to shot), and the amplification factor was found to be less than $1.75\times$ in all cases. This shows that amplification is significantly reduced at reduced density even when the seed wavelength is adjusted to maintain the resonance. The observation is consistent with a rapid decrease of the SRS amplification rate as density is decreased, which is expected from linear calculations of SRS gain in which the amplification drops exponentially as the wave damping rate increases, and the wave damping rate increases rapidly as the density decreases due to an increasing Debye length. The observation of amplification only with the 1200 nm wavelength seed and not with the 1124 nm seed, is also consistent with the dramatically higher unseeded SRS measured at the long wavelength as shown in Fig. 3.

IV. CONCLUSIONS

In conclusion, these experiments are the first demonstration of the amplification of a resonant 1 ps seed pulse by stimulated Raman scattering in the plasma produced by, and coexisting with, a 1 ns long pump beam. The plasma density was kept low so that strong inverse bremsstrahlung absorption is minimized even when the plasma scale is increased to the several cm size needed for efficient pulse compression of the 1 ns beam. Under these conditions energy amplification

factors of the seed beam of as much as $37\times$ were achieved at the highest beam intensities. This observation demonstrates that the linear SRS process needed for pulse compression is active under plasma conditions achievable for pulse compression, and transfers significant energy from the pump to the seed in these conditions. Experiments with different pump and seed intensity, plasma density, and seed wavelength, further confirm the amplification occurs at a resonant density determined by the frequency difference of the beams and that it increases significantly as both the resonant density and intensity are increased under these conditions.

ACKNOWLEDGMENTS

This work was performed under the auspices of the U.S. Department of Energy by Lawrence Livermore National Laboratory under Contract No. DE-AC52-07NA27344.

- ¹M. Tabak, J. Hammer, M. E. Glinsky, W. L. Kruer, S. C. Wilks, J. Woodworth, E. M. Campbell, M. D. Perry, and R. J. Mason, *Phys. Plasmas* **1**, 1626 (1994).
- ²D. C. Eder, P. Amendt, and S. C. Wilks, *Phys. Rev. A* **45**, 6761 (1992).
- ³T. Tajima and J. M. Dawson, *Phys. Rev. Lett.* **43**, 267 (1979); E. Esarey, P. Sprangle, J. Krall, and A. Ting, *IEEE Trans. Plasma Sci.* **24**, 252 (1996), and references therein.
- ⁴G. A. Mourou, C. P. J. Barty, and M. D. Perry, *Phys. Today* **51**(1), 22 (1998).
- ⁵V. M. Malkin, G. Shvets, and N. J. Fisch, *Phys. Rev. Lett.* **82**, 4448 (1999).
- ⁶G. Shvets, N. J. Fisch, A. Pukhov, and J. Meyer-ter-Vehn, *Phys. Rev. Lett.* **81**, 4879 (1998).
- ⁷Y. Ping, W. Chen, and S. Suckewer, *Phys. Rev. Lett.* **92**, 175007 (2004).
- ⁸M. Dreher, E. Takahashi, J. Meyer-ter-Vehn, and K. J. Witte, *Phys. Rev. Lett.* **93**, 095001 (2004).
- ⁹W. Cheng, Y. Avitzour, Y. Ping, S. Suckewer, N. J. Fisch, M. S. Hur, and J. S. Wurtele, *Phys. Rev. Lett.* **94**, 045003 (2005).
- ¹⁰A. A. Balakin, G. M. Fraiman, and N. J. Fisch, *JETP Lett.* **80**, 12 (2004).
- ¹¹P. Mounaix, D. Pesme, W. Rozmus, and M. Casanova, *Phys. Fluids B* **5**, 3304 (1993).
- ¹²V. M. Malkin and N. J. Fisch, *Phys. Plasmas* **12**, 044507 (2005).
- ¹³S. N. Dixit, J. K. Lawson, K. R. Manes, H. T. Powell, and K. A. Nugent, *Opt. Lett.* **19**, 417 (1994).
- ¹⁴V. Malka, C. Coulaud, J. P. Geindre, V. Lopez, Z. Najmudin, D. Neely, and F. Amiranoff, *Rev. Sci. Instrum.* **71**, 2329 (2000); S. Semushin and V. Malka, *ibid.* **72**, 2961 (2001).
- ¹⁵M. M. Marinak, G. D. Kerbel, N. A. Gentile, O. Jones, D. Munro, S. Pollaine, T. R. Dittrich, and S. W. Haan, *Phys. Plasmas* **8**, 2275 (2001).
- ¹⁶G. Gregori, S. H. Glenzer, J. Knight, C. Niemann, D. Price, D. H. Froula, M. J. Edwards, R. P. J. Town, A. Brantov, W. Rozmus, and V. Yu. Bychenkov, *Phys. Rev. Lett.* **92**, 205006 (2004).